IJARSCT

International Journal of Advanced Research in Science, Communication and Technology

International Open-Access, Double-Blind, Peer-Reviewed, Refereed, Multidisciplinary Online Journal

ISSN: 2581-9429 Volume 6, Issue 1, September 2026 Impact Factor: 8.2

Design of a Five-dimension digital-twin layout model for a Modular Battery-Assembly Plant

Dr. Arvind A R[1], Mr. Nagamanikkam N[1], Ms. Vaddula Suvidha[1], Mr. Chinnadurai J[1], Dr. R. Murugan[2], Mr. Mahesh Swaminathan[2], Mr. Deepak P[2]

[1]Ashok Leyland, Chennai

[2] Panimalar Engineering College, Chennai, Tamil Nadu, India

ara.arvind@gmail.com[1]

Abstract: *The electrification of road transport is expanding demand for dedicated battery-pack assembly capacity, and manufacturers increasingly seek to design, verify and rebalance such lines virtually before committing capital. This paper reports the design of a digital-twin layout for a modular cell-to-module-to-pack (C2M2P) assembly plant for a prismatic lithium-iron-phosphate (LFP) electric-vehicle battery pack of 3.2 V per cell, sixteen cells per module (16S) and three modules per pack (3S). A three-dimensional virtual entity was built in DELMIA against the actual two-dimensional plant layout and organised as a five-dimension digital-twin model comprising physical entity, virtual entity, twin data, services and connections [9,10]. A provenance-labelled data layer classifies every quantity as source-derived, engineering-reference, calculated or estimated, so that confirmed project data is not conflated with assumptions — the manual analogue of the data-integrity discipline that full digital twins enforce at scale. A discrete-event throughput model localises the line constraint to the cell-stacking robot (≈30 modules h⁻¹) and the six-axis busbar-welding station (≈55 modules h⁻¹); a gravitational-load and NIOSH-based ergonomic screening justifies overhead handling for the 64 kg module and 192 kg pack; and a qualitative failure-mode assessment maps dominant risks to design mitigations. The study shows how a defensible, service-oriented digital-twin layout can be specified from incomplete concept-stage data, and it defines the connections that must be instrumented to advance the model from a digital shadow to a fully closed-loop twin [13].*

Keywords: Digital twin • Plant layout design • Modular battery assembly • Electric-vehicle battery pack • DELMIA • Discrete-event simulation • Bottleneck analysis • Industry 4.0

I. INTRODUCTION

The transition from internal-combustion to battery-electric mobility is now a structural feature of the automotive industry, and national policy in large emerging markets explicitly targets high electric-vehicle (EV) penetration in commercial fleets within the decade [66]. Because the traction battery accounts for a large share of an EV's cost and mass, the pack is simultaneously an electrical, thermal, structural and safety-critical subsystem, and the assembly system that builds it must reconcile all four requirements in a single production flow [47,52]. At the architectural level the industry is consolidating around fewer, larger prismatic cells and toward cell-to-module (C2M) and cell-to-pack (C2P) integration to raise gravimetric and volumetric efficiency [52,53], with lithium-iron-phosphate (LFP) chemistries dominant for cost- and safety-sensitive applications owing to their thermal stability and long cycle life [54,55].

Translating such an architecture into hardware requires controlled cell and module handling, adhesive dispensing and curing, busbar joining (predominantly laser welding for prismatic terminals [50,51]), module compression and strapping, and a sequence of electrical and pneumatic tests. As line complexity and capital intensity rise, manufacturers increasingly wish to design, verify and rebalance these lines *virtually* before physical commissioning. The digital twin — a virtual model kept in correspondence with a physical asset through data [1,3,5] — has become the reference paradigm for this ambition, and its five-dimension formulation (physical entity, virtual entity, services, twin data and connections) provides a concrete engineering structure for building one [9,10]. In battery production specifically, digital twins are being applied across the value chain to raise yield, cut scrap and shorten ramp-up [41,42,43,44,45].

Despite this momentum, most published battery work addresses either the finished pack or a single unit process, while most digital-twin-for-layout work is demonstrated on generic machining or assembly cells rather than on a battery line built from a real plant drawing. Comparatively little connects the two at the concept-and-CAD stage, where design data is necessarily incomplete. The present study addresses that gap. Building on a CAD-based station-level design developed in a commercial-vehicle manufacturer's project-planning office, it specifies a digital-twin layout for a complete C2M2P assembly plant and makes four contributions: (i) it instantiates the five-dimension digital-twin model concretely for a modular battery line; (ii) it embeds a provenance-labelled twin-data layer that keeps confirmed data separate from assumptions; (iii) it uses a discrete-event throughput model within the virtual entity to localise the line bottleneck; and (iv) it links a gravitational-load/ergonomic analysis and a failure-mode assessment to the twin's service layer. The scope is explicitly design and analysis: no physical build, live data feed or finite-element validation is claimed.

Fig. 1 Reference prismatic LFP cell used throughout the study: nominal 3.2 V, ≈4 kg — the fundamental building block of the 16-cell module and 48-cell pack.

II. RELATED WORK

2.1 Digital-twin concept, models and classification

The digital-twin idea originates with Grieves, who framed a physical product, a virtual product and the bidirectional data linking them [1], later elaborated for complex-system behaviour with Vickers [2]; Glaessgen and Stargel introduced the paradigm to aerospace vehicle health management [3]. Tao and co-workers extended Grieves' three-part construct into a five-dimension model — physical entity, virtual entity, services, twin data and connections — that has become the dominant engineering reference for building twins [4,8,9,10], and popularised the vision of pervasive twinning [5]. Comprehensive surveys map the state of the art [7,12,16,17,18], its enabling technologies [9], modelling practice [10], data methods [79] and its relationship to cyber-physical systems and Industry 4.0 [8,14]. Kritzinger et al. provide the classification the field has converged on, distinguishing a digital *model* (no automated data exchange), a digital *shadow* (automated one-way physical→virtual flow) and a digital *twin* (automated bidirectional flow) [13]; this taxonomy is central to the maturity assessment in Sect. 5. Systematic reviews by Jones et al. [15], Semeraro et al. [22] and Liu et al. [17], together with modelling-perspective analyses [20,21] and predictive formulations at scale [19], frame the open challenges of fidelity, data quality and closed-loop control that this study confronts at concept stage.

2.2 Digital twins for factory layout, shop-floor and assembly lines

Within manufacturing, digital twins have been applied to shop-floor management and control [4,32,33], rapid line reconfiguration [30,39], geometry assurance in assembly [31], decision support [35] and overall smart-manufacturing system design [25]. Boschert and Rosen [77] and Schleich et al. [78] emphasise simulation and a consistent product/production model as the twin's backbone. For layout specifically, Choi and Kim propose a framework that couples optimisation, simulation and a digital twin for intelligent factory layout design [26], while Nafors et al. demonstrate hybrid digital twins for factory-layout planning using scanned as-is data [27]. Discrete-event simulation (DES) is the workhorse behind these layout twins: reviews document its central role in modelling dynamic material flow and identifying bottlenecks [36,38], line-balancing case studies quantify its value [37], and DES-driven layout optimisation has been reported to raise capacity and cut work-in-progress substantially [40]. Sun et al. show online DES analytics improving assembly-flow-line throughput in a twin setting [28], and Talkhestani et al. address the

IJARSCT
International Journal of Advanced Research in Science, Communication and Technology
International Open-Access, Double-Blind, Peer-Reviewed, Refereed, Multidisciplinary Online Journal
ISSN: 2581-9429 Volume 6, Issue 1, September 2026 Impact Factor: 8.2

synchronisation problem — keeping virtual and physical consistent through anchor points — that separates a shadow from a true twin [29]. Data-driven twin frameworks [23] and DES–twin integration challenges [36] complete the methodological backdrop for Sect. 5.

2.3 Digital twins in battery and electric-vehicle production

Digital twins are being adopted across the battery value chain. Reviews of EV-battery digital twins catalogue use cases spanning raw material, cell and pack manufacturing, in-service operation, second life and recycling, and identify manufacturing quality assurance as a dominant driver [43]. In cell manufacturing, dedicated studies establish data-management and traceability foundations [42] and enumerate concrete twin use cases from a gigafactory cost perspective [41]. Recent work extends twins to battery management and charging optimisation [44,46] and to an AI-plus-simulation synthesis across the whole battery lifecycle [45]. In parallel, the pack-assembly literature that this study draws on documents the underlying unit processes: modular and reusable pack construction [47], structural adhesive bonding and its end-of-life penalty [48,49], laser and hybrid welding of tab-to-busbar interconnections [50,51], cell/pack format trade-offs [52], cell-to-body structural integration [53], LFP cell selection and fast-charge architecture [54,55], pack thermal management [56,57,58,59,60], assembly-process FMEA [61] and assembly automation [65]. Ergonomic-intervention studies on vehicle-assembly lines [62,63,64] motivate the manual-handling analysis. Against this backdrop, the contribution here is integrative: assembling these process facts into a single, service-oriented digital-twin layout grounded in a real modular-plant drawing.

III. THE PHYSICAL MODULAR BATTERY-ASSEMBLY PLANT

The physical entity is a modular C2M2P assembly plant for a prismatic LFP EV pack. The reference cell (Fig. 1) has a nominal voltage of 3.2 V and a mass of ≈4 kg; sixteen cells in series form a 51.2 V module and three modules in series form a 153.6 V pack (Fig. 2). The plant is modular in two senses relevant to a layout twin: the *product* is built up in discrete, repeated module blocks, and the *line* is organised as self-contained stations — module line M10–M190 and pack line P10–P140 — each of which can be modelled, duplicated or rebalanced independently in the virtual layout. This modularity is what makes the plant a natural candidate for a reconfigurable digital twin [30,39]. Because cell capacity was not stated in the project material it was estimated from cell mass and a representative prismatic-LFP specific-energy band of 140–170 Wh kg^{-1} [54]; at the mid-band 155 Wh kg^{-1} the cell energy is ≈620 Wh, giving an estimated capacity of ≈195 Ah that propagates deterministically to module and pack level (Table 1). A gravimetric cross-check closes the model: 29 952 Wh / 192 kg ≈ 156 Wh kg^{-1}, consistent with the 155 Wh kg^{-1} assumed at cell level.

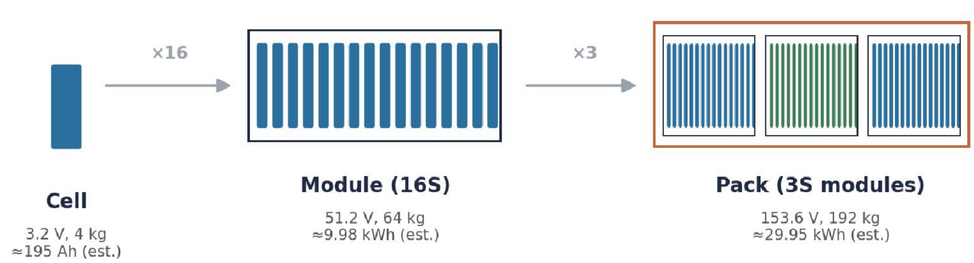

Fig. 2 Cell-to-module-to-pack build-up: 16 series cells form a 51.2 V module; three series modules form a 153.6 V, ≈29.95 kWh pack. Voltage, mass and quantities are source-derived; capacity and energy are engineering estimates.

DOI: 10.48175/IJARSCT-38256

IJARSCT
International Journal of Advanced Research in Science, Communication and Technology
International Open-Access, Double-Blind, Peer-Reviewed, Refereed, Multidisciplinary Online Journal
ISSN: 2581-9429 Volume 6, Issue 1, September 2026 Impact Factor: 8.2

Table 1 Cell/module/pack configuration and electrical summary held in the twin-data layer. Voltage, mass and quantities are source-derived; capacity and energy are engineering estimates derived from the specific-energy band.

Level	Voltage	Capacity*	Energy*	Mass / W = mg
Single cell	3.2 V	≈195 Ah	≈620 Wh	4 kg / 39.24 N
Module (16S)	51.2 V	≈195 Ah	≈9.98 kWh	64 kg / 627.84 N
Pack (3S)	153.6 V	≈195 Ah	≈29.95 kWh	192 kg / 1883.52 N

**Capacity and energy require confirmation against the manufacturer cell datasheet; every downstream figure that depends on capacity inherits this estimate and would be rescaled once the datasheet value is available.*

IV. THE DIGITAL-TWIN LAYOUT FRAMEWORK

The layout twin is organised as the five-dimension model MDT = (PE, VE, Ss, DD, CN) of Tao et al. [9,10], instantiated for this plant in Fig. 3 and Table 2. The **physical entity (PE)** is the modular line of Sect. 3 with its conveyors, KBK cranes, six-axis welders, gluing and test stations and their sensors. The **virtual entity (VE)** is the DELMIA three-dimensional replica of that line, built from the two-dimensional plant drawing and carrying geometry, reach envelopes, a discrete-event throughput model, and the ergonomic and structural relations used for analysis. The **services (Ss)** layer turns the model into decisions — bottleneck localisation, layout re-balancing, cycle-time and KPI dashboards, ergonomic screening, what-if capacity planning, virtual commissioning and design-for-recycling checks. The **twin data (DD)** layer fuses these under the provenance convention of Table 3, and the **connections (CN)** bind the dimensions together.

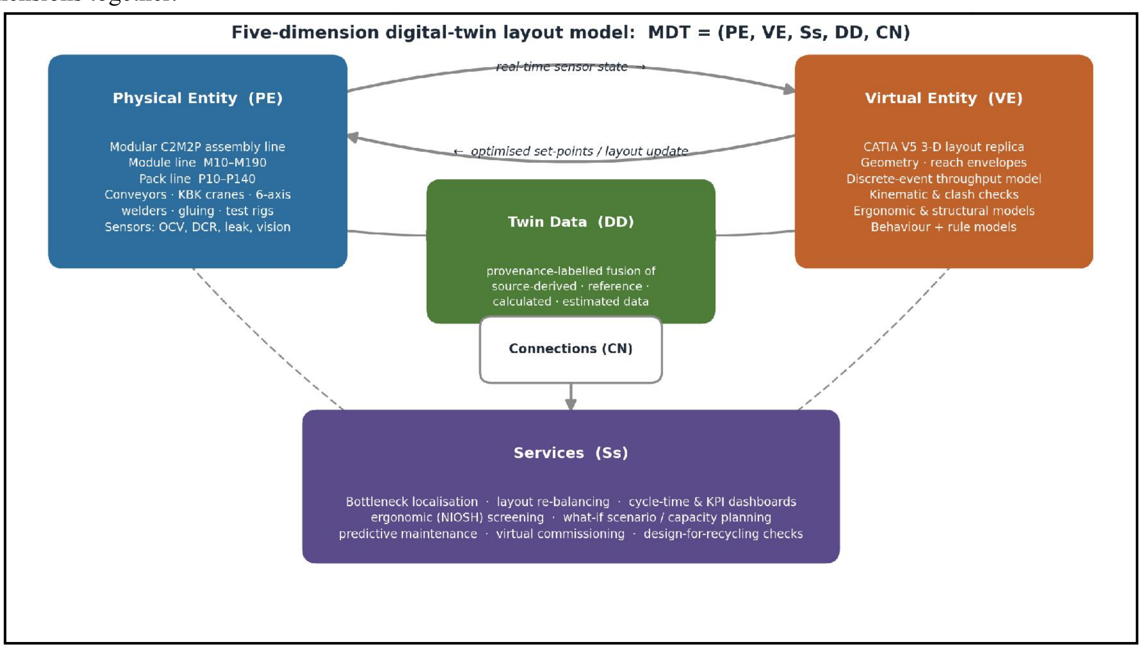

Fig. 3 Five-dimension digital-twin layout model MDT = (PE, VE, Ss, DD, CN) instantiated for the modular battery-assembly plant. At concept stage the physical→virtual link is a manual (digital-model / shadow) flow; the dashed connections mark links to be instrumented to reach a closed-loop twin.

IJARSCT
International Journal of Advanced Research in Science, Communication and Technology
International Open-Access, Double-Blind, Peer-Reviewed, Refereed, Multidisciplinary Online Journal
ISSN: 2581-9429
Volume 6, Issue 1, September 2026
Impact Factor: 8.2

Table 2 The five digital-twin dimensions instantiated for the modular battery-assembly plant.

Dimension	Symbol	Instantiation in this study	Primary data source
Physical entity	PE	Modular line M10–M190 and P10–P140; conveyors, KBK cranes, six-axis welders, gluing, compression, test rigs	Plant layout drawing; project material
Virtual entity	VE	DELMIA 3-D replica; DES throughput model; kinematic/clash, ergonomic and structural models	CAD build; engineering models
Services	Ss	Bottleneck localisation, layout re-balancing, KPI dashboards, NIOSH screening, what-if planning, virtual commissioning	Derived analyses (Sect. 6)
Twin data	DD	Provenance-labelled fusion of source-derived, reference, calculated and estimated quantities	Table 3 convention
Connections	CN	PE↔VE state/set-point flow; PE/VE↔DD; DD↔Ss (manual at concept stage; sensor-fed in target state)	OCV, DCR, leak, vision sensors

4.1 The twin-data (provenance) layer

Because concept-stage industrial data is inherently incomplete, a full digital twin's value depends less on any single number than on the *integrity* of its data layer [23,79]. This study therefore attaches a four-level provenance label to every quantity (Table 3), letting a reader distinguish a confirmed project value from an engineering-reference band, a deterministic calculation or an illustrative assumption. Where a value was absent it was estimated transparently from first principles and flagged, rather than silently invented. This convention is the manual, small-scale analogue of the traceability that MES-backed battery-production twins enforce automatically [42,45], and it is what allows the model to remain useful before datasheet values are released.

Table 3 Data-provenance labelling convention applied to every quantity in the twin-data layer.

Label	Meaning	Example in this study
Source-derived	Confirmed value recorded in the industrial project material	Cell voltage 3.2 V; 16 cells/module; 3 modules/pack; 4 kg cell mass
Engineering reference	Established handbook/standard value used where a project value is absent	LFP specific energy 140–170 Wh kg^{-1}; NIOSH ≈23 kg lift limit
Calculated	Derived deterministically from source or reference inputs	Module weight $W = mg = 627.8$ N; 51 weld joints per pack
Estimated / assumed	Illustrative value adopted to demonstrate a method, flagged for confirmation	Adhesive bead 3 mm × 1.5 mm; weld time 3 s per joint

V. MATERIALS AND METHODS

5.1 Building the virtual entity in DELMIA

All CAD work was carried out in DELMIA (Dassault Systèmes) using the Part Design and Assembly Design workbenches [70]. Twenty-five station- and equipment-level components — frames, trays, fixtures, enclosures, manipulator links, the moving conveyor, the six-axis welding cell, the KBK overhead crane and the cell-stacking robot — were modelled from sketched profiles and combined into station assemblies with coincidence, contact and offset

IJARSCT
International Journal of Advanced Research in Science, Communication and Technology
International Open-Access, Double-Blind, Peer-Reviewed, Refereed, Multidisciplinary Online Journal
ISSN: 2581-9429
Volume 6, Issue 1, September 2026
Impact Factor: 8.2

constraints, then arranged to match the two-dimensional plant layout (Fig. 4). Representative virtual-entity concepts are shown in Fig. 6. Interference was checked visually within each assembly, and degrees-of-freedom and reach-envelope reasoning was applied to the robot and crane; no formal DMU-Kinematics motion simulation was executed, and this limitation is stated explicitly. In digital-twin terms the artefact produced is at this stage a high-fidelity digital *model / shadow* rather than a closed-loop twin [13,27].

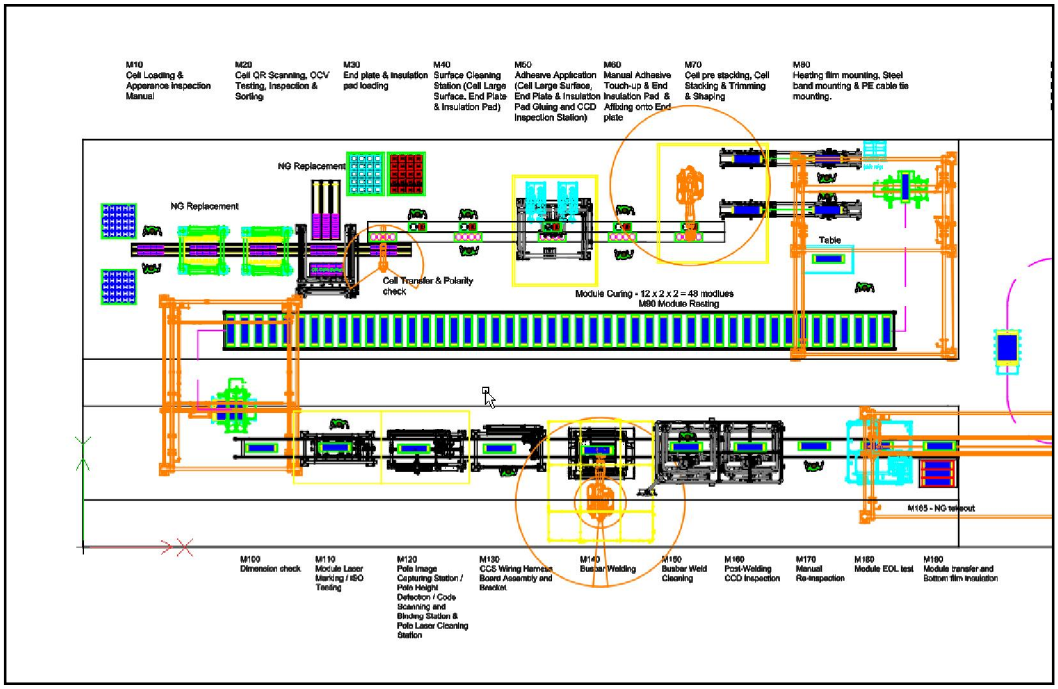

Fig. 4 Two-dimensional plant layout of the battery-module assembly line (stations M10–M190), the primary reference the virtual entity replicates. Call-outs identify cell loading and OCV/QR screening, insulation-pad and end-plate loading, adhesive application and cell stacking, the M90 module-curing zone (12 × 2 × 2 = 48 modules), dimension checking, laser marking, busbar welding and end-of-line testing.

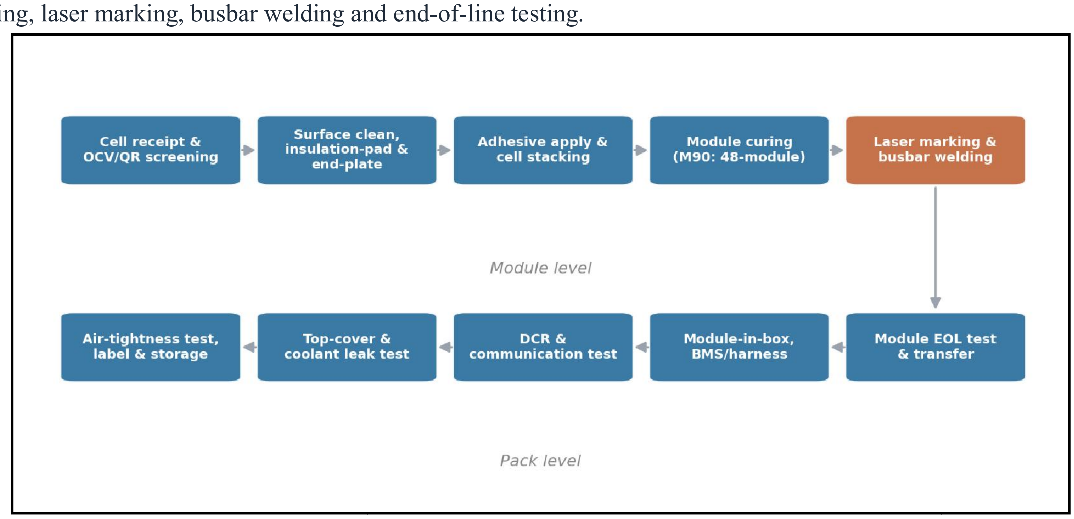

IJARSCT
International Journal of Advanced Research in Science, Communication and Technology
International Open-Access, Double-Blind, Peer-Reviewed, Refereed, Multidisciplinary Online Journal
ISSN: 2581-9429
Volume 6, Issue 1, September 2026
Impact Factor: 8.2

Fig. 5 Connected manufacturing flow abstracted from the module- and pack-line layouts and encoded as the discrete-event routing of the virtual entity. The busbar-welding step (highlighted) is one of the two throughput-limiting operations identified in Sect. 6.1.

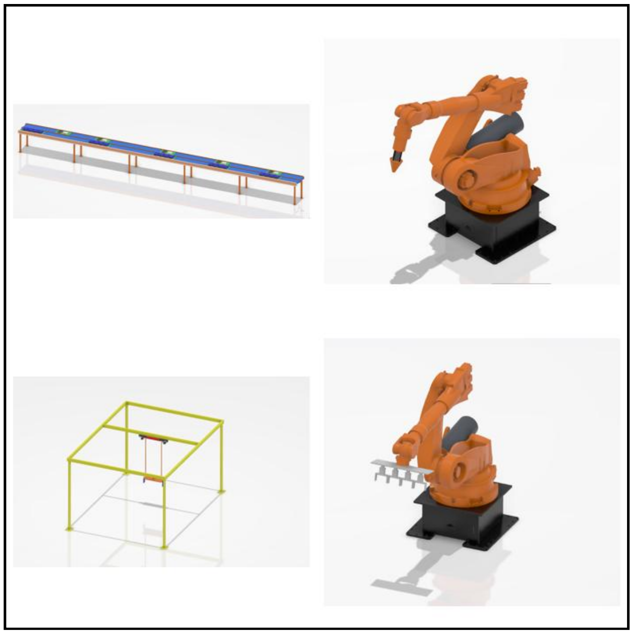

Fig. 6 Representative DELMIA virtual-entity concepts: (top-left) cell/module moving conveyor; (top-right) six-axis robotic busbar-welding concept; (bottom-left) KBK overhead crane for module transfer; (bottom-right) cell pre-stacking/stacking/trimming/shaping robot with rake end-effector.

5.2 Discrete-event throughput model and analysis services

Each station's process description was converted into an estimated cycle time, combining fixed quantities that follow deterministically from the 16 × 3 configuration with clearly-labelled assumed process times, following standard DES practice for manufacturing lines [36,37,38]. For example, a 16-series module requires $n - 1 = 15$ inter-cell busbar joints plus two terminal joints — 17 welds per module and 51 per pack (a fixed quantity) — so with an assumed 3 s weld time and a 15 s indexing overhead the welding cycle is 66 s per module (≈55 modules h^{-1}). The same method was applied to cell stacking, gluing, compression/strapping, laser marking/ISO testing, OCV/QR screening, air-tightness and DCR/communication testing (Table 4). Four analysis services were then defined on the virtual entity: (i) a C2M2P electrical/mass model with an internal specific-energy cross-check; (ii) a station-level throughput and bottleneck service; (iii) a gravitational-load and manual-handling-energy service benchmarked against the revised NIOSH lifting equation [69]; and (iv) a qualitative failure-mode-and-effects (FMEA) service following the risk-prioritisation logic of recent battery-assembly FMEA work [61].

Table 4 Station-level cycle-time and throughput summary (the DES input encoded in the virtual entity). Fixed quantities follow from the confirmed 16 × 3 configuration; process times are engineering assumptions flagged for confirmation.

Station	Governing quantity	Cycle time	Throughput	Level
Cell stacking/trim/shape robot	7.5 s/cell × 16	120 s/module	≈30 mod h^{-1}	Module
Six-axis busbar welding	17 welds × 3 s + 15 s	66 s/module	≈55 mod h^{-1}	Module

IJARSCT

International Journal of Advanced Research in Science, Communication and Technology

International Open-Access, Double-Blind, Peer-Reviewed, Refereed, Multidisciplinary Online Journal

ISSN: 2581-9429 Volume 6, Issue 1, September 2026 Impact Factor: 8.2

Station	Governing quantity	Cycle time	Throughput	Level
Gluing (module)	7.2 mL bead + index	40.8 s/module	≈88 mod h^{-1}	Module
OCV / QR screening	2.0 s/cell × 16	32 s/module	≈112 mod h^{-1}	Module
Compression / strapping	18 s dwell	18 s/module	≈200 mod h^{-1}	Module
Laser marking / ISO test	mark + scan + dwell	12.1 s/module	≈297 mod h^{-1}	Module
Bottom-cover glue robot	36 mL @ 20 mL min^{-1}	108 s/pack	≈33 pack h^{-1}	Pack
Air-tightness (leak) test	30 s hold + 10 s	40 s/pack	≈90 pack h^{-1}	Pack
DCR / communication test	handshake + pulse	10 s/pack	≈360 pack h^{-1}	Pack

VI. RESULTS

6.1 Bottleneck localisation service

Figure 7 plots the estimated module-level throughput of each station. The two slowest operations are the cell pre-stacking/stacking/trimming/shaping robot (≈30 modules h^{-1}) and the six-axis welding station (≈55 modules h^{-1}); every other module-level station offers three- to ten-fold higher nominal capacity, and the pack-level test stations are faster still. Under the modelled assumptions the line is therefore stacking- and welding-limited, and these two stations are the rational targets for cycle-time reduction or duplication if higher rates are required — precisely the kind of layout decision a twin's service layer exists to support [26,28,40]. The finding is robust to the weakest assumptions: the 51 weld joints per pack are fixed by the configuration, so only the assumed 3 s weld time and 15 s overhead move the welding bar, and halving either would still leave welding among the two slowest stations. The result also corrects an intuitive but incorrect expectation that material handling would dominate — handling and inspection stations, though numerous, are rarely the constraint [65].

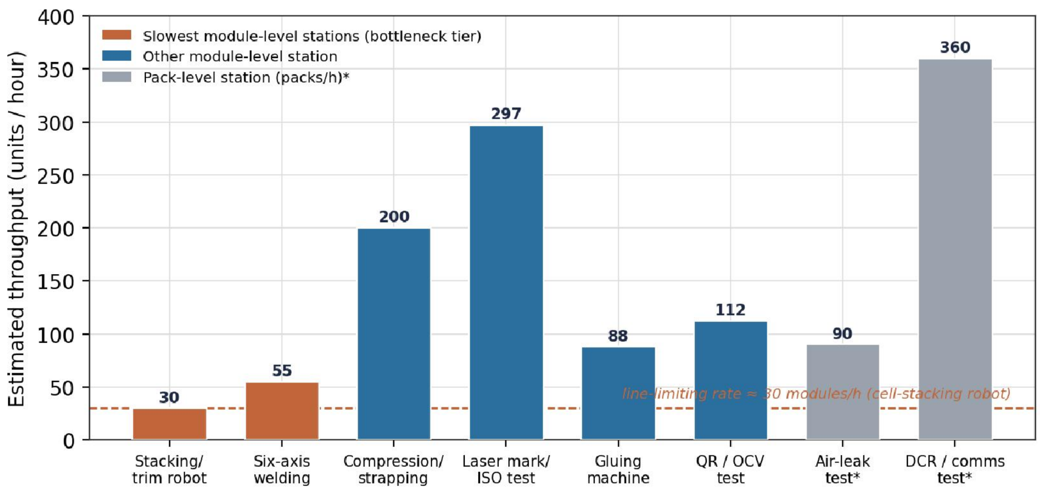

Fig. 7 Estimated per-station throughput reported by the bottleneck service. The cell-stacking robot and six-axis welding station (highlighted) are the two slowest module-level operations; pack-level test stations (grey) are shown in packs h^{-1} for context. All process times are labelled assumptions pending confirmation.

The electrical-test set-points scale deterministically with the series-cell count and therefore double as commissioning targets held in the twin. Applying Ohm's law with an assumed 0.4 mΩ cell internal resistance and a 10 A test current, the direct-current resistance rises from 0.4 mΩ (4 mV) at cell level to 6.4 mΩ (64 mV) per module and 19.2 mΩ

DOI: 10.48175/IJARSCT-38256

(192 mV) per pack (Fig. 8). Because DCR scales linearly with the $16 \times 3 = 48$ series-cell count, any future change to the series/parallel arrangement rescales the target by the same rule — an example of how the provenance-labelled twin remains useful even before the datasheet resistance is confirmed.

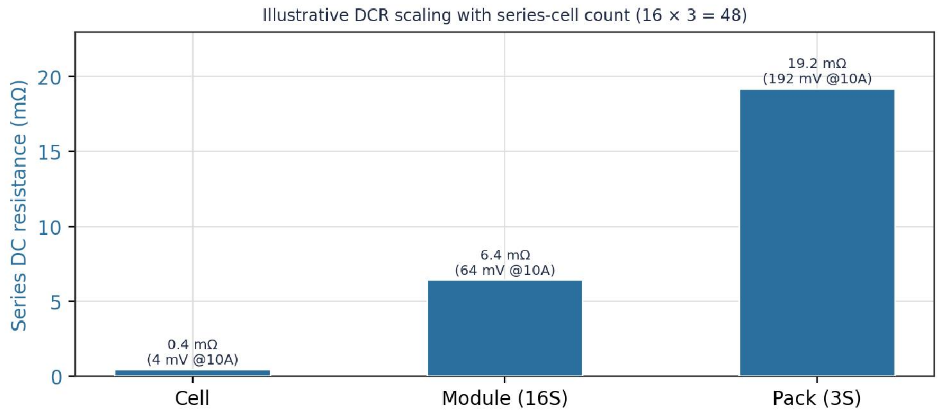

Fig. 8 Illustrative direct-current-resistance (DCR) scaling from cell to pack at a 10 A test current, using an assumed 0.4 mΩ cell resistance. The linear rise with series-cell count gives the twin a checkable commissioning target for the DCR test station.

6.2 Ergonomic-screening service

The gravitational load on any handled item is W = mg with $g = 9.81\ m\,s^{-2}$; across the confirmed masses the single cell, module and pack carry 39.24 N, 627.84 N and 1883.52 N respectively (Fig. 9). The module-curing (M90) zone, dimensioned by the layout to $12 \times 2 \times 2 = 48$ modules, implies a supported load of ≈30.1 kN, flagging the curing structure as a priority for detailed structural verification [67,68]. The decisive ergonomic result, however, is the load ceiling: the revised NIOSH lifting equation recommends a load constant of order 23 kg for a single unassisted lift [69], which sits far below both the 64 kg module and the 192 kg pack — a factor of roughly three to eight over the recommended range. Manual handling of a complete module or pack is therefore outside the guideline, which is why the overhead KBK cranes and the bottom-cover trolley are load-bearing design necessities rather than conveniences. This quantitative link from a first-principles ergonomic limit to a specific equipment decision mirrors the intervention logic of recent vehicle-assembly ergonomics studies [62,63,64], and the ergonomic-screening service makes it an explicit, auditable output of the twin.

IJARSCT
International Journal of Advanced Research in Science, Communication and Technology
International Open-Access, Double-Blind, Peer-Reviewed, Refereed, Multidisciplinary Online Journal
ISSN: 2581-9429
Volume 6, Issue 1, September 2026
Impact Factor: 8.2

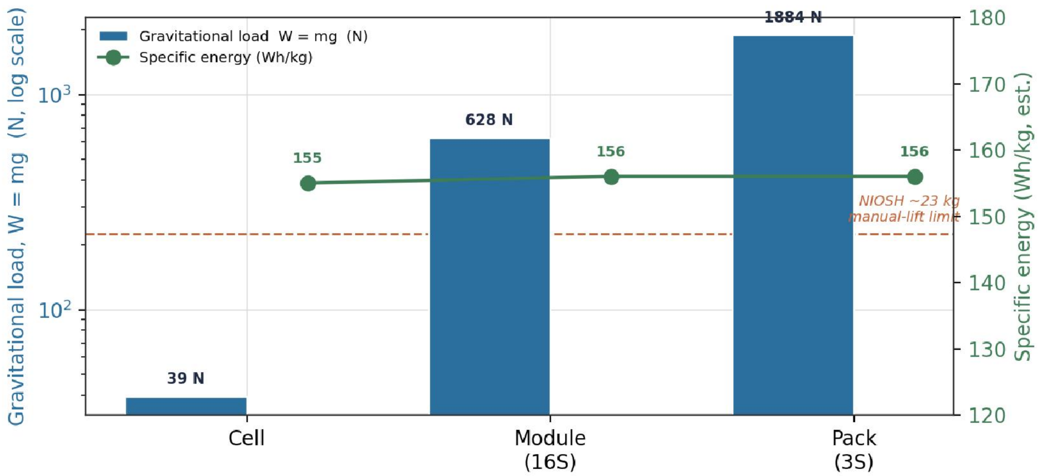

Fig. 9 Gravitational load W = mg at cell, module and pack level (bars, log scale) with the pack-level specific-energy check (line). The ≈23 kg NIOSH single-person lifting limit (dashed) lies far below the module and pack loads, justifying the overhead-handling equipment.

6.3 Failure-mode service and twin-maturity assessment

A qualitative FMEA service connects dominant failure modes to design mitigations across three families — mechanical (frame deflection, fastener loosening, conveyor misalignment, bearing wear), process (mis-transfer, mis-positioning, adhesive under/over-application, jams) and battery-specific (impact or case damage, insulation damage, short-circuit or measurement faults) — rated on a High/Medium/Low scale (Table 5) [61]. The conveyor and robotic-handling concepts exist precisely to remove manual movement of cells and modules and so reduce impact and mishandling risk, while the intrinsic thermal stability of LFP lowers the consequence of a mechanical insult relative to other chemistries [54]. Finally, Table 6 assesses each subsystem against the Kritzinger integration levels [13]: today every connection is a manual digital model or, where a sensor already exists (OCV, DCR, leak, vision), a potential digital shadow; reaching a closed-loop twin requires instrumenting the physical→virtual and virtual→physical connections marked as targets, and it is these connections — not further geometry — that define the remaining work.

Table 5 Qualitative failure-mode-and-effects summary exposed by the FMEA service (engineering assessment; S = severity, O = occurrence, D = detection, on a High/Medium/Low scale).

System	Failure mode	S / O / D	Mitigation (design intent)
Moving conveyor	Belt/roller misalignment	M / M / M	Guarding, presence sensors, planned maintenance
KBK crane / trolley	Load-attachment slip	H / L / M	Rated hoist, secure attachment, safe-load limits
Gluing / compression / strapping	Adhesive or strap-tension variation	M / M / M	Controlled dispensing/compression, inspection step
Laser marking / ISO station	Laser exposure to operator	H / L / M	Enclosure, interlocks, restricted access
DCR / OCV / leak test stations	Faulty connection or seal	M–H / L–M / M	Fixture design, grounding, pass/fail interlock

IJARSCT
International Journal of Advanced Research in Science, Communication and Technology
International Open-Access, Double-Blind, Peer-Reviewed, Refereed, Multidisciplinary Online Journal
ISSN: 2581-9429
Volume 6, Issue 1, September 2026
Impact Factor: 8.2

System	Failure mode	S / O / D	Mitigation (design intent)
Storage racks / gantry	Overload / instability	H / L / L–M	Load- and CG-based design, rated-capacity confirmation

Table 6 Digital-twin integration maturity (after Kritzinger et al. [13]) per subsystem — current state achievable from concept-stage data versus the target state and the connection that must be instrumented.

Subsystem	Current level	Target level	Enabling connection to instrument
Six-axis welding cell	Digital model	Digital twin	Weld count/time + quality feedback → rebalance
Cell-stacking robot	Digital model	Digital twin	Cycle-time & jam telemetry → rate control
OCV / DCR / leak tests	Digital shadow	Digital twin	Live pass/fail + set-point write-back
Conveyor & KBK handling	Digital model	Digital shadow	Position/interlock sensing → flow sync
M90 curing zone	Digital model	Digital shadow	Occupancy + dwell timers → WIP tracking

VII. DISCUSSION

Three results carry engineering significance beyond the individual concepts.

Embedding a discrete-event throughput model in the virtual entity localises the line constraint to the cell-stacking and busbar-welding stations, giving a data-grounded priority for any capacity increase; this is the canonical layout-twin service reported in the literature [26,28,40], here demonstrated on a real battery-line drawing rather than a generic cell.

The ergonomic service converts a generic safety principle into a specific, auditable equipment decision by benchmarking module and pack masses against the NIOSH limit [62,63,64,69]. Third, and most importantly for a twin, the provenance-labelled data layer shows that a single transparent estimate can propagate consistently through the whole model while remaining honestly labelled — the manual analogue of the data-integrity discipline that MES-backed battery twins enforce automatically [23,42,45,79].

The design also embodies trends the literature independently supports: reliance on structural adhesive aligns with production practice while inheriting the disassembly penalty a design-for-recycling revision must weigh [48,49]; the six-axis laser-welding concept matches the consensus on prismatic-terminal joining [50,51]; and the integrated coolant leak test reflects the centrality of liquid cooling to pack thermal management [56,57,59,60].

The limitations follow directly from the concept stage and from the Kritzinger taxonomy [13]: what has been built is a high-fidelity digital model/shadow, not yet a closed-loop twin. No kinematic or finite-element validation was run; structural grades and load ratings are provisional; and every throughput and set-point figure that depends on an assumed process time or the estimated cell capacity must be re-evaluated once released specifications and live sensor streams are connected.

VIII. CONCLUSION AND FUTURE SCOPE

This paper has specified a digital-twin layout for a modular cell-to-module-to-pack battery-assembly plant for a prismatic LFP EV pack of 3.2 V/16S/3S architecture. Working from an actual industrial plant drawing, a DELMIA virtual entity of twenty-five station concepts was organised as a five-dimension digital-twin model with a provenance-labelled data layer, and four analysis services were defined on it. The throughput service localised the constraint to the cell-stacking (≈30 modules h^{-1}) and welding (≈55 modules h^{-1}) stations; the ergonomic service justified overhead handling against the ≈23 kg NIOSH limit for the 64 kg module and 192 kg pack; and the FMEA and maturity services mapped risks and integration gaps to concrete design and instrumentation actions. The principal contribution is methodological: a defensible, service-oriented digital-twin layout can be specified from incomplete concept-stage data provided the provenance of every quantity is explicit.

Future work follows from the maturity assessment of Table 6: (i) instrument the physical→virtual and virtual→physical connections so the model advances from digital shadow to closed-loop twin [13,29]; (ii) build and run DMU-Kinematics mechanisms for the welding robot and KBK crane with automated clash detection; (iii) couple the discrete-event model to live station telemetry for online rebalancing [28,40]; (iv) confirm the cell datasheet so all capacity-dependent set-points, adhesive volumes and weld counts can be rescaled; and (v) extend the twin toward energy, thermal and design-for-recycling services across the pack lifecycle [45,49].

Declarations

Conflict of interest: The authors declare no competing interests.

Data availability: The plant layout and CAD models underlying this study are part of confidential industrial project material and are not publicly available; the derived calculations are fully reproduced in the paper.

Acknowledgements: The authors thank the manufacturer for internship and guidance during the CAD-development work on which this study is based.

REFERENCES

1. Grieves M (2014) Digital twin: manufacturing excellence through virtual factory replication. White Paper, Florida Institute of Technology, pp 1–7

2. Grieves M, Vickers J (2017) Digital twin: mitigating unpredictable, undesirable emergent behaviour in complex systems. In: Transdisciplinary Perspectives on Complex Systems. Springer, Cham, pp 85–113. https://doi.org/10.1007/978-3-319-38756-7_4

3. Glaessgen EH, Stargel DS (2012) The digital twin paradigm for future NASA and US Air Force vehicles. In: 53rd AIAA/ASME/ASCE/AHS/ASC Structures, Structural Dynamics and Materials Conference. https://doi.org/10.2514/6.2012-1818

4. Tao F, Zhang M (2017) Digital twin shop-floor: a new shop-floor paradigm towards smart manufacturing. IEEE Access 5:20418–20427. https://doi.org/10.1109/ACCESS.2017.2756069

5. Tao F, Qi Q (2019) Make more digital twins. Nature 573:490–491. https://doi.org/10.1038/d41586-019-02849-1

6. Tao F, Cheng J, Qi Q, Zhang M, Zhang H, Sui F (2018) Digital twin-driven product design, manufacturing and service with big data. Int J Adv Manuf Technol 94(9–12):3563–3576. https://doi.org/10.1007/s00170-017-0233-1

7. Tao F, Zhang H, Liu A, Nee AYC (2019) Digital twin in industry: state-of-the-art. IEEE Trans Ind Inform 15(4):2405–2415. https://doi.org/10.1109/TII.2018.2873186

8. Tao F, Qi Q, Wang L, Nee AYC (2019) Digital twins and cyber–physical systems toward smart manufacturing and Industry 4.0: correlation and comparison. Engineering 5(4):653–661. https://doi.org/10.1016/j.eng.2019.01.014

9. Qi Q, Tao F, Hu T, Anwer N, Liu A, Wei Y, Wang L, Nee AYC (2021) Enabling technologies and tools for digital twin. J Manuf Syst 58:3–21. https://doi.org/10.1016/j.jmsy.2019.10.001

10. Tao F, Xiao B, Qi Q, Cheng J, Ji P (2022) Digital twin modeling. J Manuf Syst 64:372–389. https://doi.org/10.1016/j.jmsy.2022.06.015

11. Tao F, Zhang M, Nee AYC (2019) Digital Twin Driven Smart Manufacturing. Academic Press, London

12. Tao F, Zhang H, Zhang C (2024) Advancements and challenges of digital twins in industry. Nat Comput Sci 4:169–177. https://doi.org/10.1038/s43588-024-00603-w

13. Kritzinger W, Karner M, Traar G, Henjes J, Sihn W (2018) Digital twin in manufacturing: a categorical literature review and classification. IFAC-PapersOnLine 51(11):1016–1022. https://doi.org/10.1016/j.ifacol.2018.08.474

14. Negri E, Fumagalli L, Macchi M (2017) A review of the roles of digital twin in CPS-based production systems. Procedia Manuf 11:939–948. https://doi.org/10.1016/j.promfg.2017.07.198
15. Jones D, Snider C, Nassehi A, Yon J, Hicks B (2020) Characterising the digital twin: a systematic literature review. CIRP J Manuf Sci Technol 29:36–52. https://doi.org/10.1016/j.cirpj.2020.02.002
16. Cimino C, Negri E, Fumagalli L (2019) Review of digital twin applications in manufacturing. Comput Ind 113:103130. https://doi.org/10.1016/j.compind.2019.103130
17. Liu M, Fang S, Dong H, Xu C (2021) Review of digital twin about concepts, technologies, and industrial applications. J Manuf Syst 58:346–361. https://doi.org/10.1016/j.jmsy.2020.06.017
18. Lu Y, Liu C, Wang KIK, Huang H, Xu X (2020) Digital twin-driven smart manufacturing: connotation, reference model, applications and research issues. Robot Comput Integr Manuf 61:101837. https://doi.org/10.1016/j.rcim.2019.101837
19. Kapteyn MG, Pretorius JVR, Willcox KE (2021) A probabilistic graphical model foundation for enabling predictive digital twins at scale. Nat Comput Sci 1:337–347. https://doi.org/10.1038/s43588-021-00069-0
20. Rasheed A, San O, Kvamsdal T (2020) Digital twin: values, challenges and enablers from a modeling perspective. IEEE Access 8:21980–22012. https://doi.org/10.1109/ACCESS.2020.2970143
21. Wagg DJ, Worden K, Barthorpe RJ, Gardner P (2020) Digital twins: state-of-the-art and future directions for modelling and simulation in engineering dynamics applications. ASCE-ASME J Risk Uncertain Eng Syst Part B Mech Eng 6(3):030901. https://doi.org/10.1115/1.4046739
22. Semeraro C, Lezoche M, Panetto H, Dassisti M (2021) Digital twin paradigm: a systematic literature review. Comput Ind 130:103469. https://doi.org/10.1016/j.compind.2021.103469
23. Friederich J, Francis DP, Lazarova-Molnar S, Mohamed N (2022) A framework for data-driven digital twins of smart manufacturing systems. Comput Ind 136:103586. https://doi.org/10.1016/j.compind.2021.103586
24. Errandonea I, Beltrán S, Arrizabalaga S (2020) Digital twin for maintenance: a literature review. Comput Ind 123:103316. https://doi.org/10.1016/j.compind.2020.103316
25. Leng J, Wang D, Shen W, Li X, Liu Q, Chen X (2021) Digital twins-based smart manufacturing system design in Industry 4.0: a review. J Manuf Syst 60:119–137. https://doi.org/10.1016/j.jmsy.2021.05.011
26. Choi SH, Kim BS (2024) Intelligent factory layout design framework through collaboration between optimization, simulation, and digital twin. J Intell Manuf. https://doi.org/10.1007/s10845-024-02340-3
27. Nafors D, Johansson B, Gullander P, Erixon S (2020) Simulation in hybrid digital twins for factory layout planning. In: 2020 Winter Simulation Conference (WSC). IEEE, pp 1619–1630. https://doi.org/10.1109/WSC48552.2020.9383908
28. Sun H, Li C, Fang X, Gu H (2017) Optimized throughput improvement of assembly flow line with digital twin online analytics. In: 2017 IEEE Int Conf on Robotics and Biomimetics (ROBIO), pp 1833–1837. https://doi.org/10.1109/ROBIO.2017.8324685
29. Talkhestani BA, Jazdi N, Schloegl W, Weyrich M (2018) Consistency check to synchronize the digital twin of manufacturing automation based on anchor points. Procedia CIRP 72:159–164. https://doi.org/10.1016/j.procir.2018.03.166
30. Leng J, Liu Q, Ye S, Jing J, Wang Y, Zhang C, Zhang D, Chen X (2020) Digital twin-driven rapid reconfiguration of the automated manufacturing system via an open architecture model. Robot Comput Integr Manuf 63:101895. https://doi.org/10.1016/j.rcim.2019.101895
31. Söderberg R, Wärmefjord K, Carlson JS, Lindkvist L (2017) Toward a digital twin for real-time geometry assurance in individualized production. CIRP Ann 66(1):137–140. https://doi.org/10.1016/j.cirp.2017.04.038
32. Zhuang C, Liu J, Xiong H (2018) Digital twin-based smart production management and control framework for the complex product assembly shop-floor. Int J Adv Manuf Technol 96:1149–1163. https://doi.org/10.1007/s00170-018-1617-6

33. Zhang H, Zhang G, Yan Q (2019) Digital twin-driven cyber-physical production system towards smart shop-floor. J Ambient Intell Humaniz Comput 10:4439–4453. https://doi.org/10.1007/s12652-018-1125-4
34. Uhlemann THJ, Lehmann C, Steinhilper R (2017) The digital twin: realizing the cyber-physical production system for Industry 4.0. Procedia CIRP 61:335–340. https://doi.org/10.1016/j.procir.2016.11.152
35. Kunath M, Winkler H (2018) Integrating the digital twin of the manufacturing system into a decision support system for improving the order management process. Procedia CIRP 72:225–231. https://doi.org/10.1016/j.procir.2018.03.192
36. Agalianos K, Ponis ST, Aretoulaki E, Plakas G, Efthymiou O (2020) Discrete event simulation and digital twins: review and challenges for the manufacturing sector. Procedia Manuf 51:1636–1641. https://doi.org/10.1016/j.promfg.2020.10.228
37. Zupan H, Herakovic N (2015) Production line balancing with discrete event simulation: a case study. IFAC-PapersOnLine 48(3):2305–2311. https://doi.org/10.1016/j.ifacol.2015.06.431
38. Qiao D, Wang Y (2021) A review of the application of discrete event simulation in manufacturing. J Phys Conf Ser 1802(2):022066. https://doi.org/10.1088/1742-6596/1802/2/022066
39. Zhang C, Xu W, Liu J, Liu Z, Zhou Z, Pham DT (2019) A reconfigurable modeling approach for digital twin-based manufacturing system. Procedia CIRP 83:118–125. https://doi.org/10.1016/j.procir.2019.03.141
40. Guo H, Zhu Y, Zhang Y, Ren Y, Chen M, Zhang R (2021) A digital twin-based layout optimization method for discrete manufacturing workshop. Int J Adv Manuf Technol 112:1307–1318. https://doi.org/10.1007/s00170-020-06568-0
41. Use cases for digital twins in battery cell manufacturing (2024). In: Towards Sustainable Customization: Bridging Smart Products and Manufacturing Systems. Lecture Notes in Mechanical Engineering. Springer, Cham. https://doi.org/10.1007/978-3-031-18318-8_82
42. Kies AD, Krauß J, Schmetz A, Baum C, Schmitt RH, Brecher C (2021) Der digitale Zwilling in der Batteriezellfertigung. wt Werkstattstechnik online 111(5):286–290. https://doi.org/10.37544/1436-4980-2021-05-20
43. Digital twin of electric vehicle battery systems: comprehensive review of the use cases, requirements, and platforms (2023). Renewable and Sustainable Energy Reviews (Elsevier)
44. Leveraging digital twin technology for battery management: a case study review (2025). IEEE Access 13. https://doi.org/10.1109/ACCESS.2025.3531833
45. Revolutionizing batteries based on digital twin through AI-simulation synergy for design, manufacturing, operation and recycling (2025). National Science Open (Science Press)
46. Liu C, Liu R, Liu X (2026) A digital twin framework for intelligent electric vehicle charging optimization in smart manufacturing systems. Appl Energy 406:127281 (Elsevier). https://doi.org/10.1016/j.apenergy.2025.127281
47. Albrecht R, et al (2025) Manufacturing and assembly of modular and reusable EV battery for environment-friendly and lightweight mobility. In: Transport Transitions — Advancing Sustainable and Inclusive Mobility (TRA 2024), Lecture Notes in Mobility. Springer, Cham. https://doi.org/10.1007/978-3-031-89444-2_37
48. Adhesive bonding in automotive battery pack manufacturing and dismantling: a review (2025). Discover Mech Eng (Springer Nature). https://doi.org/10.1007/s44245-025-00107-5
49. Seiler T, et al (2026) Light electric vehicle battery pack design for an improved circular economy using detachable cell contacting. Springer Fachmedien Wiesbaden. https://doi.org/10.1007/978-3-658-50502-8_11
50. Tab-to-busbar interconnections in EV battery packs: an introductory review of typical welding methods (2025). Micromachines 17(1):2 (MDPI). https://doi.org/10.3390/mi17010002
51. Agarwal A, et al (2025) Controlled mixing of Al and Cu in laser-welded joints with combined use of core/ring beams and oscillation for EV battery pack applications. Opt Laser Technol 192:113718 (Elsevier)
52. Design and production trade-offs in lithium-ion batteries from cell formats to electric vehicles (2026). Cell Reports Physical Science (Cell Press/Elsevier)

53. A review of cell-to-body (CTB) battery-structure integration design for electric vehicles (2026). Front Mech Eng. https://doi.org/10.3389/fmech.2026.1825484
54. Yeganehdoust F, Madikere Raghunatha Reddy AK, Zaghib K (2025) Cell architecture design for fast-charging lithium-ion batteries in electric vehicles. Batteries 11(1):20 (MDPI). https://doi.org/10.3390/batteries11010020
55. Akyildiz A, et al (2025) Optimum selection of lithium iron phosphate battery cells for electric vehicles. IEEE Access 13:55070–55080. https://doi.org/10.1109/ACCESS.2025.3553081
56. Zhu H, Chakir C, Shi P, Hai B (2026) Power battery thermal management systems in electric vehicle: a comprehensive review. Proc IMechE Part D: J Automobile Eng (SAGE). https://doi.org/10.1177/09544070251381862
57. Murugan M, et al (2025) A comprehensive review of thermal management methods and ideal system design for improved electric vehicle battery pack performance and safety. Energy Sci Eng (Wiley). https://doi.org/10.1002/ese3.2081
58. A review on thermal management system and employed biomimetic technology to enhance lithium-ion battery packs for electric vehicles (2025). J Energy Storage (Elsevier)
59. Enhancing thermal stability in prismatic lithium-ion battery pack in electric vehicle through optimization for an indirect liquid-cooling system (2025). J Comput Des Eng 12(3):51 (Oxford University Press)
60. Pujari HK, et al (2025) Integrated thermal and battery management for electric vehicles: experimental validation and simulation-based optimization of lithium-ion batteries. Energy Explor Exploit (SAGE). https://doi.org/10.1177/01445987251337094
61. A risk analysis method for potential failure modes in the lithium-ion battery assembly process based on optimized FMEA and DHHFLTS (2025). Sci Rep 15:28327 (Springer Nature). https://doi.org/10.1038/s41598-025-12681-5
62. Ergonomic interventions to improve musculoskeletal disorders among vehicle assembly workers: a one-year longitudinal study (2025). BMC Public Health 25 (Springer Nature). https://doi.org/10.1186/s12889-025-21798-1
63. Sharma NK, Tiwari M, Thakur A, Ganguli AK (2025) Evaluating biomechanical risks in manual material handling: an ergonomic intervention approach. Ergonomics (Taylor & Francis). https://doi.org/10.1080/00140139.2025.2473678
64. Prevalence and multivariate analysis of risk factors associated with musculoskeletal disorders among automotive assembly workers: a cross-sectional study (2025). BMC Public Health 25:2710 (Springer Nature). https://doi.org/10.1186/s12889-025-23987-4
65. Automation of operations in assembly of battery modules in electric vehicles (2024). IFAC-PapersOnLine (INCOM 2024, Elsevier)
66. India Brand Equity Foundation (2026) Electric vehicle industry in India: growth, trends and policy. IBEF Industry Report. https://www.ibef.org/industry/electric-vehicle
67. Budynas RG, Nisbett JK (2020) Shigley's Mechanical Engineering Design, 11th edn. McGraw-Hill Education, New York
68. Bureau of Indian Standards. IS 2062: Hot rolled medium and high tensile structural steel — specification. BIS, New Delhi
69. Waters TR, Putz-Anderson V, Garg A (1994) Applications manual for the revised NIOSH lifting equation. DHHS (NIOSH) Publication 94-110, U.S. Department of Health and Human Services
70. Dassault Systèmes. CATIA V5 product documentation — Part Design, Assembly Design and DMU Kinematics user guides. Dassault Systèmes SE
71. Lee J, Bagheri B, Kao HA (2015) A cyber-physical systems architecture for Industry 4.0-based manufacturing systems. Manuf Lett 3:18–23. https://doi.org/10.1016/j.mfglet.2014.12.001
72. Monostori L (2014) Cyber-physical production systems: roots, expectations and R&D challenges. Procedia CIRP 17:9–13. https://doi.org/10.1016/j.procir.2014.03.115
73. Kagermann H, Wahlster W, Helbig J (2013) Recommendations for implementing the strategic initiative INDUSTRIE 4.0: final report of the Industrie 4.0 Working Group. acatech, Frankfurt

74. Zhong RY, Xu X, Klotz E, Newman ST (2017) Intelligent manufacturing in the context of Industry 4.0: a review. Engineering 3(5):616–630. https://doi.org/10.1016/J.ENG.2017.05.015

75. Xu X, Lu Y, Vogel-Heuser B, Wang L (2021) Industry 4.0 and Industry 5.0 — inception, conception and perception. J Manuf Syst 61:530–535. https://doi.org/10.1016/j.jmsy.2021.10.006

76. Leng J, Sha W, Wang B, et al (2022) Industry 5.0: prospect and retrospect. J Manuf Syst 65:279–295. https://doi.org/10.1016/j.jmsy.2022.09.017

77. Boschert S, Rosen R (2016) Digital twin — the simulation aspect. In: Mechatronic Futures. Springer, Cham, pp 59–74. https://doi.org/10.1007/978-3-319-32156-1_5

78. Schleich B, Anwer N, Mathieu L, Wartzack S (2017) Shaping the digital twin for design and production engineering. CIRP Ann 66(1):141–144. https://doi.org/10.1016/j.cirp.2017.04.040

79. Zhang M, Tao F, Huang B, Liu A, Wang L, Anwer N, Nee AYC (2024) Digital twin data: methods and key technologies. Digital Twin 1:2. https://doi.org/10.12688/digitaltwin.17467.2

80. Zhang H, Li Y, Zhang S, et al (2025) Artificial intelligence-enhanced digital twin systems engineering towards the industrial metaverse in the era of Industry 5.0. Chin J Mech Eng 38:40. https://doi.org/10.1186/s10033-025-01210-0